# Reconstruction of three-dimensional auroral ionospheric conductivities via an assimilative technique

*McGranaghan et al.* [2015a, b], [2016], [2016b, In prep.]


Ryan McGranaghan[1], Delores J. Knipp[1,2], Tomoko Matsuo[3], Ellen Cousins[4], Stan Solomon[2]

[1]University of Colorado Boulder - Boulder, CO
[2]High Altitude Observatory, National Center for Atmospheric Research - Boulder, CO
[3]Cooperative Institute for Research in the Environmental Sciences - Boulder, CO
[4]Weather Analytics – Bethesda, MD

Email: ryan.mcgranaghan@colorado.edu


## Key Findings

- New optimal interpolation technique reconstructs conductivities in two- and three-dimensions
- Improved global conductivity distributions bring SuperDARN and AMPERE data into closer agreement, especially during geomagnetically active periods
- 2D and 3D specification of conductivity reveal new understanding of the solar wind-magnetosphere-ionosphere system and emphasize importance of analyzing ionosphere in 3D

## Introduction

We address a key barrier to system science for the magnetosphere-ionosphere-thermosphere (MIT) system, ionospheric conductivity. The ionospheric conductivity plays a crucial role in regulating MIT system response to dynamic geospace behavior.

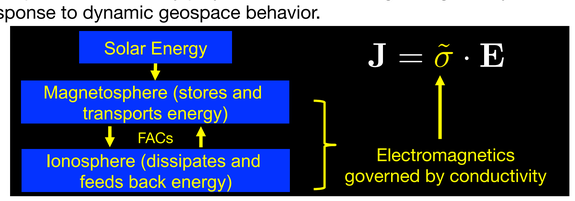


However, in the past global specification of ionospheric conductivity required significant simplifying assumptions:

Often integrated over altitude (e.g. conductance)

$$\tilde{\sigma} \rightarrow \int_h \sigma_x \mathrm{d}h = \Sigma_x$$

Precipitating particles assumed to have simple Maxwellian energy distribution and conductances governed by *Robinson et al.* [1987] formulas

$$\Sigma_P = \frac{40\bar{E}}{16 + \bar{E}^2}\Phi_E^{1/2}$$
$$\frac{\Sigma_H}{\Sigma_P} = 0.45(\bar{E})^{0.85}$$

Such modeling difficulties have contributed to significant gaps in our understanding of processes in the MIT system. We overcome these assumptions to produce the first characterization of primary modes of ionospheric conductivity variability as Empirical Orthogonal Functions (EOFs) and create a new optimal interpolation technique to estimate complete high-latitude conductivity fields, in 2D and 3D. We show that the optimally-interpolated fields yield better agreement between ground- and space-based data and allow better estimation of high-latitude electrodynamics. Our results emphasize the importance of analyzing the ionosphere in 3D.

## Optimal Interpolation (OI) Technique

Reconstruction of complete high-latitude conductivities via optimal interpolation (OI)

Follows technique developed by *Richmond and Kamide* [1988] (AMIE), *Matsuo et al.* [2005], and *Cousins et al.* [2013]

Objective: Optimally combine information from **observations** and a **background model**, taking into account **error properties** of both

**Background model**: EOF-based mean (see next section)
**Observations**: DMSP particle precipitation data
**Error properties**:

- For background model: Estimated from EOFs
- For DMSP particle precipitation data: Poisson statistics for individual spectra

$$\vec{x}_a = \vec{x}_b + K\left(\vec{y} - H\vec{x}_b\right)$$
$$K = P_b H^{\mathrm{T}}\left(H P_b H^{\mathrm{T}} + R\right)$$

$\vec{x}_a$ – Analysis field
$\vec{x}_b$ – Background model
$K$ – Kalman gain
$\vec{y}$ – Observations
$H$ – Forward operator
$P_b$ – Background model error covariance
$R$ – Observational error covariance

Visually:

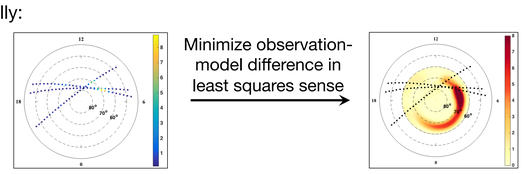


## Importance of Analyzing Ionosphere in 3D: Empirical Orthogonal Functions

**EOF Process**

1. **Directly-measured electron energy spectra** from Defense Meteorological Satellite Program (DMSP) satellites F6-F8 and F16-F18 are used to characterize auroral ionization sources
2. **GLobal AirglOW (GLOW) model** [*Solomon et al.*, 1988] + conductivity (GLOWcon) [*McGranaghan et al.*, 2015a] solves 2-stream electron transport to yield conductivity profiles
3. **EOFs spread sparse information into global picture** by deconstructing the Hall and Pedersen residual fields into a few dominant modes of variability (2D fields to the right [*McGranaghan et al.*, 2015b] and 3D fields below [*McGranaghan et al.*, 2016b, in. prep.])

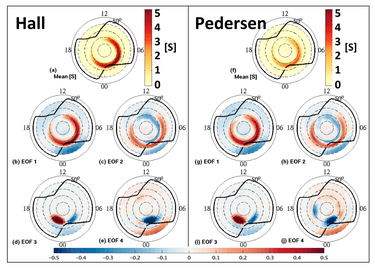


Mean fields and EOFs (time-invariant spatial fields) for Hall and Pedersen conductances (left) and conductivities (below), in magnetic coordinates. The low-latitude limit on all polar plots is 50° and dashed lines are plotted at 10° increments up to 80°. The solid black curves indicate the boundaries of observational support.

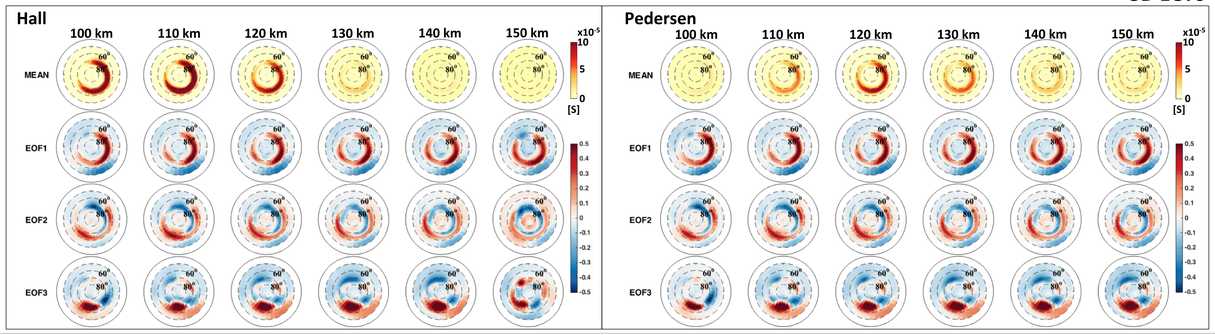


## OI Conductances and Importance to Ionospheric Electrodynamics and Data Assimilation

We demonstrate the OI technique three hours into the passage of a CME on November 30 – Steady southward (-5 nT $B_Z$) IMF conditions with -5 nT $B_x$ and +5 nT $B_y$ and average solar wind velocity persisted during this period

This is the same period analyzed by *Cousins et al.* [2015b] (hereafter C2015)
We compare with the conductance models used therein - 1
OI (hereafter M2015) conductances yield:

- Better characterization of enhancements due to discrete precipitation - 2
- Closer agreement between SuperDARN and AMPERE data when used in Assimilative Mapping of Ionospheric Electrodynamics (AMIE) procedure - 3, 4, and 5
- Improved performance during geomagnetic activity - 5

McGranaghan, R., et al. (2016a), Optimal interpolation analysis of high-latitude ionospheric Hall and Pedersen conductivities: Application to assimilative ionospheric electrodynamics reconstruction, J. Geophys. Res. Space Physics, 121, doi:10.1002/2016JA022486.

1

| Conductance models compared and details | |
|---|---|
| **Auroral Conductance Model** | **Details** |
| C2015 I | Diffuse precipitation from OVATION Prime auroral precipitation model [*Newell et al.*, 2009]; no discrete precipitation; Robinson formulas used to relate electron energy flux and average energy to conductance; Background I[a] |
| C2015 II | Same as C2015 I, but with background II[b] |
| M2015 I | OI conductances using DMSP particle precipitation observations; EOF-based background covariance; Background I |
| M2015 II | Same as M2015 I, but with background II |

[a] Background I refers to night-side conductances $\Sigma_H > 0.8$ and $\Sigma_P > 0.4$
[b] Background II refers to night-side conductances $\Sigma_{H,P} > 4.0$

2

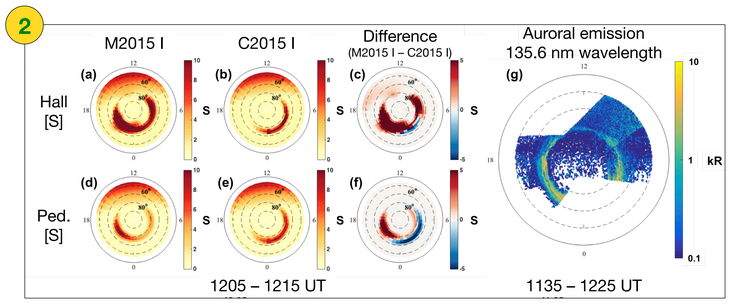


Quantitative validation of M2015 I conductances capturing discrete precipitation shown in auroral imagery from DMSP Special Sensor Ultraviolet Spectrographic Imager (SSUSI). Complete high-latitude Hall and Pedersen conductance maps for the northern hemisphere on November 30, 2011 for the time period 1205-1215 UT from the (a,d) M2015 I model, (b,e) C2015 I model, (e,f) difference (M2015 - C2015). (g) DMSP F16-F18 SSUSI 135.6 nm auroral emission data from the encapsulating time period 1135-1225 UT.

3

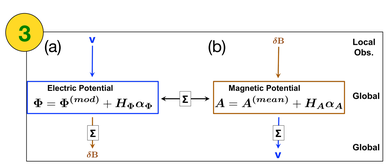


Two paths of electrodynamics estimation to compare conductance models. (a) SuperDARN to predict AMPERE (V➔δB); (b) AMPERE to predict SuperDARN (δB➔V). Anywhere a Σ lies on top of an arrow indicates knowledge of conductance is needed to relate the two parameters.

4

| | Conductance model evaluation[a] | | | | |
|---|---|---|---|---|---|
| | Median absolute deviations [m/s or nT] | | | | |
| | **Conductance Model** | **C2015 I** | **C2015 II** | **M2015 I** | **M2015 II** |
| Nov. 30 | δB ➔ V | 684.20 | 149.77 | 382.69 | 145.69 |
| | V ➔ δB | 36.88 | 39.03 | 37.03 | 39.98 |

[a] Median absolute deviation values are given for using SuperDARN to predict AMPERE (δB ➔ V) in nT and vice versa in m/s with estimated uncertainty values of ~0.2nT and ~1m/s, respectively [*Cousins et el.*, 2015b]

5

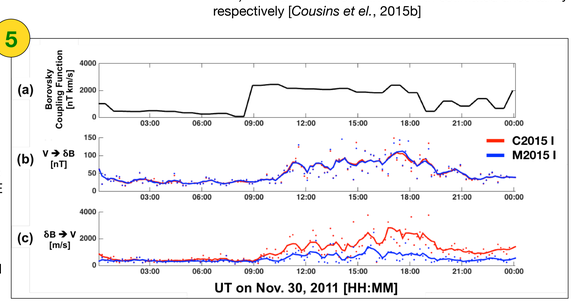


Temporal dependence of observation-prediction MADs using (b) SuperDARN to predict AMPERE (V ➔ δB) or (c) AMPERE to predict SuperDARN (δB ➔ V) for November 30, 2011. (a) The Borovsky coupling function. MADs have been binned according to time (i.e. a single MAD value was calculated from all spatial locations at a given time).

## Fundamental Conductivity Understanding

EOFs yield newly discovered relationships between solar wind-magnetosphere-ionosphere behavior, particle precipitation mapping locations, and ionospheric conductivities:

(a,b) EOF2 ⟷ IMF $B_Z$
(c) EOF3 ⟷ Poynting flux driving

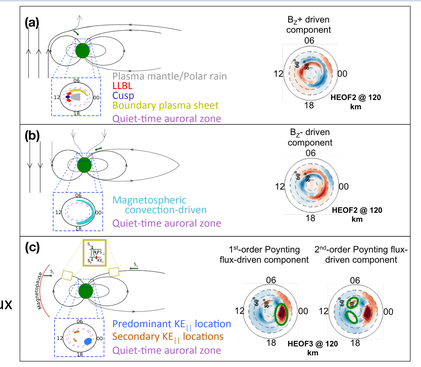


## 3D OI Conductivity

Perform the OI estimation at discrete altitudes (100-140 km @ 1200 UT shown):

**Background model**: Altitude-specific EOF-based mean
**Observations**: Altitude-specific conductivities from DMSP particle precipitation data
**Error properties**:

- For background model: Estimated from altitude-specific EOFs
- For DMSP particle precipitation data: Poisson statistics for individual spectra

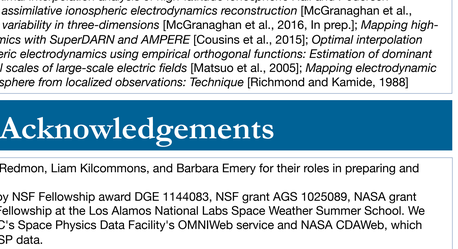


Complete high-latitude 3D (a) Hall and (b) Pedersen conductivity maps for the northern hemisphere at 1200 UT on November 30, 2011.

## Conclusions

**Ionospheric Conductivity Empirical Orthogonal Functions:**

First characterization of primary modes of ionospheric Hall and Pedersen conductance variability as EOFs [*McGranaghan et al.*, 2015b]

Extended analysis to 3D conductivities [*McGranaghan et al.*, 2016b, in prep.]

2D and 3D treatment of conductivities distinctly different

**Optimal Interpolation of Ionospheric Conductivities [*McGranaghan et al.*, 2016a]:**

New optimal interpolation technique yields complete high-latitude conductance distributions

OI technique capable of better ionospheric conductance specification, especially during geomagnetically active periods

Yields closer agreement between AMPERE and SuperDARN data

Showed significant vertical gradients in three-dimensional conductivity

**Larger Implications:**

Overcame Maxwellian assumption for precipitating particles

Better conductivity information allows consistent assimilation of ground- and space-based data

Critical to study fully 3D ionosphere

## References


*The Auroral 6300 Å emission* [Solomon et al., 1988]; *Modes of high-latitude auroral conductance variability derived from DMSP energetic electron precipitation observations: Empirical Orthogonal Function (EOF) analysis* [McGranaghan et al., 2015b], *Optimal interpolation analysis of high-latitude ionospheric Hall and Pedersen conductivities and application to assimilative ionospheric electrodynamics reconstruction* [McGranaghan et al., 2016]; *High-latitude conductivity variability in three-dimensions* [McGranaghan et al., 2016, In prep.]; *Mapping high-latitude ionospheric electrodynamics with SuperDARN and AMPERE* [Cousins et al., 2015]; *Optimal interpolation analysis of high-latitude ionospheric electrodynamics using empirical orthogonal functions: Estimation of dominant modes of variability and temporal scales of large-scale electric fields* [Matsuo et al., 2005]; *Mapping electrodynamic features of the high-latitude ionosphere from localized observations: Technique* [Richmond and Kamide, 1988]


## Acknowledgements


We gratefully acknowledge Rob Redmon, Liam Kilcommons, and Barbara Emery for their roles in preparing and using the DMSP data.
R.M.G. was partially supported by NSF Fellowship award DGE 1144083, NSF grant AGS 1025089, NASA grant NNX13AD64G, and by the Vela Fellowship at the Los Alamos National Labs Space Weather Summer School. We acknowledge use of NASA/GSFC's Space Physics Data Facility's OMNIWeb service and NASA CDAWeb, which provided the solar wind and DMSP data.